Synthesis of Elastomeric Poly(propylene) Using Unsymmetrical Zirconocene Catalysts: Marked Reactivity Differences of "Rac"- and "Meso"-like Diastereomers

Anna M. Bravakis, Linda E. Bailey, Michael Pigeon, and Scott Collins*

Department of Chemistry, University of Waterloo, Waterloo, Ontario, Canada N2L 3G1

Received September 9, 1997; Revised Manuscript Received December 3, 1997

ABSTRACT: Synthesis of "meso"- and "racemic"-like diastereomers of $Me_2Si(3\text{-}MeInd)(Ind)ZrCl_2$ (**5** and **6**, respectively) was achieved through either metathetical reactions between the dianion of $Me_2(3\text{-}MeIndH)(IndH)$ (**4**) with $ZrCl_4$ or via amine elimination reactions, followed by fractional crystallization. Propylene polymerizations using *meso*-**5** in the presence of methyl aluminoxane under a variety of conditions leads to the formation of low molecular weight, semicrystalline, low tacticity, poly(propylene) (PP). The dominant chain transfer mechanism in this case is shown to involve β-H transfer to monomer. In contrast, *rac*-**6** provides higher molecular weight, semicrystalline, elastomeric poly(propylene) (elPP) under a variety of conditions; chain transfer in this case involves, predominantly, β-H transfer to Zr. The properties of elPP produced using catalyst **6** show a gradual change from a lightly, cross-linked elastomer to a poorly crystalline thermoplastic, depending on both polymer molecular weight and crystallinity as revealed by differential scanning calorimetry and tensile testing. In particular, more crystalline material exhibits a higher initial modulus, yielding behavior and lower strain to break than less crystalline material of equivalent molecular weight. These findings further define polymer properties for the synthesis of flexible elastomers using this class of catalysts.

Introduction

The use of metallocene catalysts for the preparation of elastomeric poly(propylene) (elPP) is a topic of considerable current interest. Elastomeric poly(propylene) was first isolated by Natta and co-workers during fractionation studies of poly(propylene) (PP) prepared using first generation Ziegler−Natta catalysts.[1] Natta concluded that this material was a stereoblock form of PP in which, e.g., isotactic sequences present in polymer chains cocrystallize with similar sequences on other chains to form a physically cross-linked elastomer. Collette and co-workers at DuPont were the first to develop supported catalysts that provided access to significant quantities of this material so as to allow fundamental study of its properties.[2] More recently, Rausch, Chien, and co-workers discovered an unsymmetrical titanocene catalyst (**1**, Chart 1) that provides elPP of narrow molecular weight distribution under a variety of conditions, which, based on its solubility properties, also possesses a fairly well-defined composition.[3] We have previously reported that related catalysts **2** also provide access to elPP and have demonstrated some minimal requirements for the formation of elastomers with useful physical properties.[4] In a related development, Waymouth and co-workers have developed oscillating catalysts (e.g., **3**),[5] that provide access to elPP with distinctly different physical properties, a possible reflection of the different mechanisms for generation of isotactic sequences in these materials.[4c] Finally, in all these materials, it appears that isotactic sequences are responsible for the generation of polymer crystallinity; an alternative approach in which syndiotactic sequences are implicated has been reported recently.[6]

In our earlier work,[4] only hafnium-based catalysts (**2**, M = Hf, X = C, Si) provided polymer of sufficiently high molecular weight (MW) to impart elastomeric properties to the semicrystalline PP formed under a variety of

Chart 1

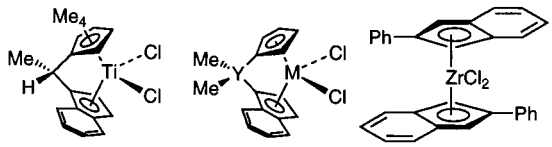

1 **2** M = Ti, Zr, Hf; Y = C, Si **3**

polymerization conditions; their zirconium analogues were much more active when activated by MAO but provided only low MW, less stereoregular material, while the titanium-based system (**2**, M = Ti, X = C) was not at all stable/active under a variety of polymerization conditions.

In this paper we describe the synthesis of a zirconium-based catalyst for the preparation of elPP, the results of some mechanistic studies concerning chain transfer in these systems, a discussion of this type of two-state catalyst, as well as some trends in the physical properties of elPP as a function of polymer crystallinity and other variables.

Results and Discussion

Metallocene Synthesis and Characterization. As mentioned above, in our earlier work, unsymmetrical zirconium catalysts (**2**, M = Zr, X = C, Si) only provided low MW, stereoirregular PP which was neither crystalline nor elastomeric.[4] We reasoned that a useful approach to the development of zirconium-based catalysts for the production of elPP would take advantage of the ongoing development of C_2-symmetric, ansa-zirconocene catalysts for the production of high MW, highly isotactic PP (i-PP). In particular, substitution patterns necessary for the production of higher MW i-PP are well documented.[7]

However, such systems would have to be desymmetrized so as to provide the minimal requirement of two

S0024-9297(97)01325-9 CCC: $15.00
Published on Web 02/03/1998

Scheme 1

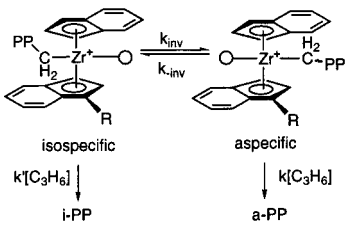

Scheme 2

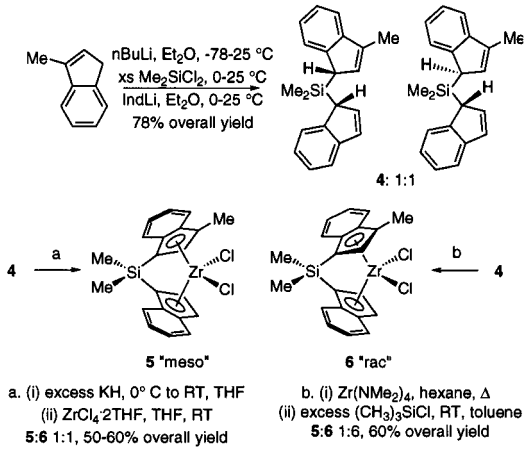

states (one aspecific, the other isopecific) for the production of crystalline and amorphous domains in the network structure of elPP.[4] Production of elPP using unsymmetrical, ansa-metallocene catalysts requires both "atactic" and isotactic sequences be present within a single polymer chain (e.g., Scheme 1[4]), and it was not obvious how one should desymmetrize a C_2-symmetric ansa-zirconocene catalyst to give an unsymmetrical system with inequivalent states of *similar* stability/reactivity so as to achieve this.

There was ample evidence in the literature that use of unsymmetrical ansa-zirconocene catalysts can provide access to highly i-PP;[8] presumably, in these cases, the two inequivalent states differ markedly in their stability or reactivity or are both isospecific (to different extents) such that i-PP is produced (vide infra).

As a first step toward the use of ansa-zirconocene catalysts for the production of elPP, a "first generation", isospecific, dimethylsilylene-bridged zirconocene catalyst (Scheme 1, R = H) could be desymmetrized by introduction of a single substitutent at the 3-position of one indenyl ring (Scheme 1, R = alkyl). By adjusting the steric size of this substitutent, one could conceivably alter the relative reactivity/stability of the two states available to this system in a controlled fashion as long as this substituent was of similar steric requirements to the six-membered ring of the unsubstituted indenyl ligand. The latter requirement is self-evident if the state on the right in Scheme 1 is to be aspecific.

The simplest member of this series, where R = Me, was selected for initial evaluation. As with related ansa-zirconocenes, two stereoisomers are possible and we have denoted these as meso (**5**: R = Me, Scheme 2) and rac (**6**: R = Me) by analogy to their C_s and C_2-symmetrical counterparts. Both are of potential interest for the preparation of elPP.

The ligand **4**, required for the synthesis of **5** and **6**, was readily prepared in high yield as a mixture of diastereomers, by the stepwise reaction of 3-methylindenyllithium with excess dimethyldichlorosilane, followed by reaction with indenyllithium as shown in Scheme 2. Conventional metathesis reaction of the potassium dianion derived from **4** with $ZrCl_4$ according to previously developed conditions[9] provided a mixture of meso and rac diastereomers (**5** and **6**, respectively) in a 1:1 ratio and in a combined yield of 50−60%. Use of the dilithio salt and/or different conditions for the metathesis reaction failed to affect this ratio. In this case, **5** is the less soluble of the two compounds formed (vide infra) and can be isolated in 15−20% overall yield by recrystallization of the mixture from toluene; the rac isomer could not be obtained in pure form using this approach.

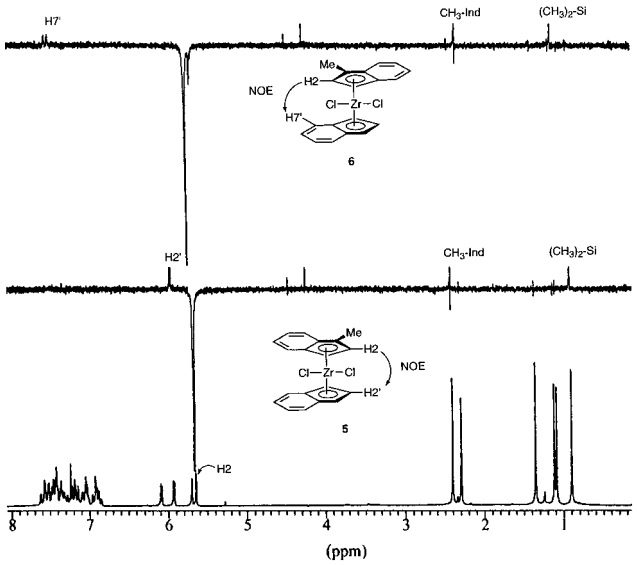

Figure 1. ^{1}H NMR NOE difference spectra for *meso*-**5** and *rac*-**6** (bridging $(CH_3)_2Si$ unit omitted for clarity), 200 MHz, 25 °C, in $CDCl_3$. ^{1}H NMR reference spectrum of a 1:1 mixture of *meso*-**5** and *rac*-**6** is shown below.

Alternatively, amine elimination reactions involving similar, symmetrical ligands and $Zr(NMe_2)_4$ have been extensively studied by Jordan and co-workers,[10] and in most cases, enhancement in rac:meso ratios is observed under thermodynamically or, in certain cases, kinetically controlled conditions. We adopted this approach for the synthesis of *rac*-**6**; in this case, amine elimination in refluxing hexane solution provided access to a mixture of bis(dimethylamido)zirconocene complexes in high yield. Treatment of this mixture with excess chlorotrimethylsilane in toluene solution gave predominantly **6** and **5** in a ratio of 6:1 from which pure **6** could be obtained by crystallization at −30 °C in 40% overall yield from silane **4**.[11]

Attempts at obtaining single crystals of either isomer, suitable for X-ray diffraction, proved fruitless—those obtained from isomer **6**, in particular, were invariably twinned, while those obtained for **5** were too small for analysis using conventional diffractometers. However, ^{1}H NMR nuclear Overhauser effect (NOE) difference spectroscopy allowed unambiguous identification of each isomer.[12] As shown in Figure 1, irradiation of the signal due to H2 in isomer **5** (which appears as a singlet in the NMR spectrum) led to measurable enhancement of the protons of the C3-methyl substituent, protons on one of the methyl groups of the silicon bridge (not shown for clarity in the chemical structures of either **5** or **6** in Figure 1), and H2′ (d, J = 3 Hz) on the other indenyl ring. Irradiation of H2 in isomer **6** led to enhancement

Table 1. Selected ^{1}H NMR Chemical Shifts and Assignments for *meso*-5 and *rac*-6[a]

Hx	*meso*-**5**	*rac*-**6**
2′	5.92 (d, 1H)	6.10 (d, 1H)
2	5.64 (s, 1H)	5.70 (s, 1H)
3′	7.04 (d, 1H)	6.91 (d, 1H)
4′, 4	7.46−7.40 (m, 2H)[b]	7.46 (m)[b,c]
5′, 5	6.91(pseudo-t, 2H)[b]	7.05 (m, 2H)[b]
6′, 6	7.18 (t, 2H)[b]	7.32 (m)[b,c]
7′, 7	7.56−7.53 (m, 2H)[b]	7.58 (dt, 1H)[d]
CH_3−Ind	2.40 (s, 3H)	2.33 (s, 3H)
$(CH_3)_2$−Si	1.35 (s, 3H), 0.90 (s, 3H)	1.11 (s, 3H), 1.08 (s, 3H)

[a] $CDCl_3$, 25 °C, 200 MHz. For a labeling Scheme see Figure 1. [b] These assignments are tentative. [c] These signals are overlapping, total integration for all protons (H7, H6, H6′, H4, H4′) is 5H. [d] This is the signal due to H7′, which has been assigned using ^{1}H NMR NOE difference spectroscopy (Figure 1).

of the corresponding signals due to the C3-methyl and one of the silicon methyl groups, but also to the aromatic proton H7′ (dt, J = 8, 1 Hz) on the opposite indenyl ring. Thus, in isomer **5**, the two protons H2 and H2′ on the different five-membered rings are in close proximity to one another, while in isomer **6**, the H2 proton on one five-membered ring is in close proximity to the H7′ aromatic proton on the other indenyl ring. As shown in Figure 1, this behavior is expected if **5** and **6** are the *meso*- and *rac*-like isomers, respectively.

^{1}H NMR spectroscopic data for **5** and **6** are summarized in Table 1; the pronounced chemical shift inequivalence of the diastereotopic methyl groups on Si in the meso isomer compared to those signals in the rac isomer is also consistent with the structural assignment based on NOE measurements. In the meso isomer, these methyl groups experience very different chemical environments (one is sandwiched between the two aromatic rings and should be deshielded relative to the other, which is only flanked by the Cp rings), while in the rac isomer the chemical environments of the two methyl groups should be very similar (each is flanked by one aromatic and one Cp ring).

Propylene Polymerization Using *meso*-5. A series of propylene polymerizations employing isomer **5** in the presence methyl aluminoxane (MAO) under various conditions were conducted and the results are summarized in Table 2, entries 1−6. Under all conditions explored, low MW (<2000 M_n), partially isotactic PP (% mmmm 20−45) was produced. Although many of these materials were semicrystalline (T_m ca. 50−80 °C), none of these polymer samples were elastomeric as would be expected based on their low MW. Although these results are qualitatively similar to those obtained using catalysts **2** (M = Zr, X = C or Si) which also provided lower MW PP, the higher stereoregularity of the polymer obtained here led to measurable crystallinity. Thus, isomer **5** meets only one of the two criteria identified for formation of elPP using unsymmetrical ansa-metallocene catalysts.[4]

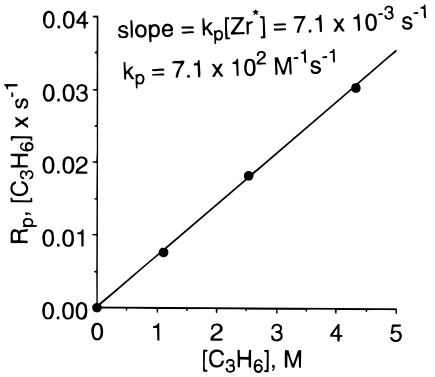

Figure 2. Effect of increasing monomer concentration on the steady-state rate of polymerization for *meso*-**5** at 25 °C.

Experiments at different monomer concentrations and constant temperature revealed that the MW (as measured independently by ^{13}C NMR analysis of end-groups and by size exclusion chromatography) was essentially insensitive to changes in monomer concentration within experimental error (Table 2, entries 1−3). In addition, the steady-state rate of polymerization, as measured by calibrated mass flow meters, exhibited changes consistent with propagation being first order in $[C_3H_6]$, as shown in Figure 2. These two findings taken together indicate that the principal mode of chain transfer in polymerizations catalyzed by isomer **5** involves β-H transfer to (coordinated) monomer (vide infra). The rather open nature of one of the lateral coordination sites in *meso*-**5** may facilitate this process which is believed to involve a six-membered cyclic transition state.[13]

Propylene Polymerization Using *rac*-6. In contrast to the results obtained using **5**, propylene polymerizations using isomer **6** provided higher MW (50−100 K M_w), partially isotactic (30−50% mmmm) PP at reasonable productivities (Table 2, entries 7−13). All of these samples had measurable crystallinity (T_m 40−

Table 2. Summary of Propylene Polymerizations with 5 and 6[a]

entry	catalyst	T_p (°C)	C_3H_6 (psi)	$[C_3H_6]$[b] (M)	A[c]	mmmm[d] (%)	M_n	M_w/M_n[f]	T_m[g] (°C)
1	**5**	25	15	1.1	640	40.7	660[e]		
2	**5**	25	30	2.5	980	37.4	740[e]		53, 73
3	**5**	25	45	4.4	1300	34.3	880[e]		49, 80
4	**5**	40	45	2.6	1300	42.1	3200[e]		53, 79
5	**5**	10	45	7.4	150	29.8	1000[e]		
6	**5**	0	45	10.9	74	22.5	910[e]		
7	**6**	0	15	2.0	1400	30.4	52 200[f]	2.20	[h]
8	**6**	25	15	1.1	1600	47.5	19 800[f]	2.62	59, 81
9	**6**	25	30	2.5	2600	37.9	28 300[f]	2.30	44, 57
10	**6**	25	45	4.4	7700	35.1	36 700[f]	2.13	49
11	**6**	40	15	0.74	1200	48.6	16 500[f]	2.24	58, 78
12	**6**	40	30	1.60	6500	46.1	25 600[f]	2.09	38, 63
13	**6**	40	45	2.63	10400	41.9	26 500[f]	2.10	43, 66
14	[i]	40	45	2.63	43600	83.0	21 300[f]	1.95	

[a] Polymerization conditions, [MAO]:[Zr] = 1000, [Zr] = 10 μM; polymerization solvent, toluene. [b] Calculated as described in the Experimental Section. [c] Catalyst activity in kg of PP/mol of Zr × h. [d] Determined by ^{13}C NMR with corrections for end groups. [e] Determined from the ^{13}C NMR spectrum as described in the Experimental Section. [f] Determined by GPC. [g] Measured by DSC. [h] No thermal transitions were detected. [i] Polymerization with *rac*-$Me_2Si(Ind)_2ZrCl_2$ under identical polymerization conditions as in entry 13.

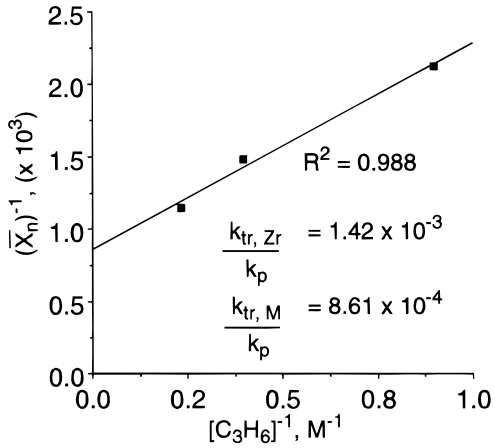

Figure 3. Relationship between $1/\bar{X}_n$ vs $[C_3H_6]^{-1}$ for *rac*-**6** at 25 °C.

80 °C) and some of these samples behaved as "classical" elastomers (vide infra).

While some of the increase in MW observed, when compared to *meso*-**5**, can be attributed to an increased rate of propagation with catalyst **6** (Table 2, e.g., entries 1−3 vs 8−10), the magnitude of the increase also suggests that chain transfer is less favorable with this catalyst under equivalent conditions. ^{13}C NMR analysis of some of the lower MW polymers produced with catalyst **6** only revealed signals consistent with chain transfer to monomer or to metal (vinylidene and *n*-propyl groups in a 1:1 ratio).

The degree of polymerization $\bar{X}_n$ is related to the ratio of the rates of propagation and chain transfer. As shown in eq 1, a plot of $1/\bar{X}_n$ vs $[M]^{-1}$ should be linear with a slope of $k_{tr,Zr}/k_p$ and intercept of $k_{tr,M}/k_p$. This relationship is depicted in Figure 3 for **6** and a comparison of these values with those estimated for **5** are summarized below (eqs 2 and 3, respectively).

$$\frac{1}{\bar{X}_n} = \frac{R_{tr}}{R_p} = \frac{k_{tr,Zr}[Zr^*] + k_{tr,M}[M][Zr^*]}{k_p[M][Zr^*]} = \frac{k_{tr,Zr}}{k_p[M]} + \frac{k_{tr,M}}{k_p} \quad (1)$$

$$1/\bar{X}_n = (1.42 \times 10^{-3})[M]^{-1} + 8.61 \times 10^{-4} \quad \text{(for } \mathbf{6}\text{)} \quad (2)$$

$$1/\bar{X}_n = (1.42 \times 10^{-2})[M]^{-1} + 4.98 \times 10^{-2} \quad \text{(for } \mathbf{5}\text{)} \quad (3)$$

It is evident that the ratios of the rate constants for chain transfer to propagation are much smaller for catalyst **6**, when compared to catalyst **5**, which is a reflection of both increased propagation rates (which differ by ∼2 under equivalent conditions, assuming equal concentrations of Zr*, Table 2) for **6** and a more pronounced decrease in chain transfer rates for **6**. Also, β-hydrogen transfer to Zr (as opposed to the monomer) dominates in the case of **6** with $k_{tr,Zr}/k_{tr,M} = 1.7$. For isomer **5**, the converse is true; chain transfer to monomer dominates over that of transfer to the metal by a factor of $k_{tr,M}/k_{tr,Zr} = 3.5$. A comparison of eqs 2 and 3 for **6** and **5**, respectively, shows that $k_{tr,Zr}/k_p$ only differs by a factor of 10 while the ratio of $k_{tr,M}/k_p$ (chain transfer to monomer) is approximately 60 times larger in the case of **5**. Both of these values are much greater than one would predict, based on activity differences alone.

Scheme 3

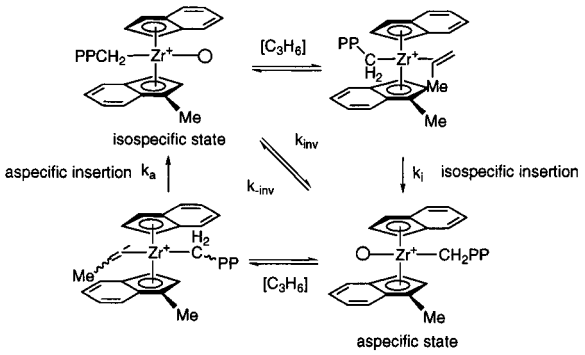

For isomer **6**, neither of the lateral coordination sites is as sterically accessible as the one (between the two C5 rings) in **5**; this is expected to have a larger influence on the rate of chain transfer to the monomer compared to chain transfer to the metal, which involves a less sterically demanding, 4-center transition state.[13] The contributing effects of steric interactions at the active metal site may be further exemplified by a comparison of entries 13 vs 14 for **6** and *rac*-$Me_2Si(Ind)_2ZrCl_2$. The introduction of the methyl group at one of the lateral sites reduces the observed activity of **6** by a factor of 4, but this is accompanied by a (slight) increase in polymer molecular weight which implies a reduction in the overall rate of chain transfer. Similar effects of substitution on MW have been noted in isospecific ansa-zirconocene catalysts.[7]

Thus, the structural properties of these isomeric but topologically different catalysts have dramatic and readily interpreted effects on polymer MW analogous to those elucidated for C_2-symmetric catalysts for the production of i-PP. This finding suggests that a great deal about what is known about these single state catalysts can be directly applied to two-state catalysts with predictable consequences. Future synthetic work will focus on this issue.

Unsymmetrical, Two-State Ansa-Zirconocene Catalysts. Comparison to Related Systems. As we have mentioned elsewhere,[4] the general features of propylene polymerization using bridged metallocene catalysts can be explained with reference to the (simplified) catalytic mechanism shown in Scheme 3. The two states available to an unsymmetrical catalyst, of the type studied here, can interconvert either through the process of migratory insertion or via inversion at the metal center, which involves migration of the polymer chain from one lateral site to the other. Unlike oscillating metallocene catalysts, which interconvert between states via the *independent* process of indenyl ring rotation,[5] the interconversion between states in systems of the sort described here is intimately related to the propagation process.

It is instructive to consider the range of behavior that would be expected from the simplified mechanism depicted in Scheme 3. One type of limiting behavior is where interconversion via chain inversion is very slow (or does not occur) compared to the rate of interconversion by the process of monomer insertion (from either state). In this case, and assuming insertion from one state is isospecific while insertion from the other is aspecific, hemi-isotactic PP would be produced. This behavior has been observed using the Zr-analogue of catalyst **1**[3d] and also in the desymmetrized, C_s-symmetric system $Me_2C(3\text{-}MeCp)(Flu)ZrCl_2$,[14] particularly

Scheme 4

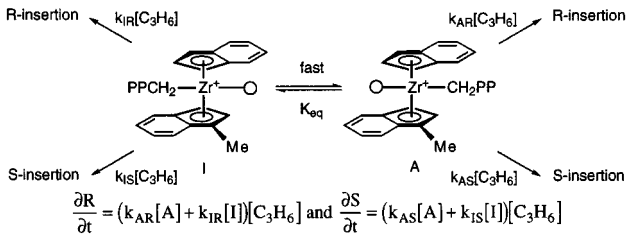

at high monomer concentrations, where alternation of insertion between the two states should be increasingly favored relative to migration of the polymer chain (vide infra).

The other kind of limiting behavior is where interconversion between states, by the process of chain migration, is very fast compared to the rate of monomer insertion (Scheme 4). This behavior corresponds to Curtin−Hammett conditions, in which the relative amounts of the two states are constant during polymerization. It can be shown that the overall probability for monomer insertion of a particular configuration (say an [R]-placement) will be constant during the lifetime of a polymer chain and will be governed by the individual stereoselectivities for insertion at the relative reactivity of and the relative stability of each state as demonstrated below.

If we define β_{tot} as the total probability for [R]-enchainment with $\beta_{tot} = \partial R/(\partial R + \partial S)$, then substitution into this expression, using the kinetic rate laws shown in Scheme 4 provides the expression shown in eq 4. Under Curtin−Hammett conditions, the stereoselectivity does not depend on experimental variables such as monomer concentration.

$$\beta_{tot} = \frac{k_{AR}[A] + k_{IR}[I]}{k_{AR}[A] + k_{IR}[I] + k_{AS}[A] + k_{IS}[I]} = \frac{k_{AR}[A] + k_{IR}[I]}{(k_{AR} + k_{AS})[A] + (k_{IR} + k_{IS})[I]} \quad (4)$$

If we define β_A and β_I as the corresponding probabilities for [R]-enchainment from the A and I states, with $\beta_A = k_{AR}/(k_{AR} + k_{AS})$ and $\beta_I = k_{IR}/(k_{IR} + k_{IS})$, then the expression shown in eq 4 simplifies to that shown in eq 5; the total stereoselectivity depends only on the instrinsic selectivity of each state, as well as the relative amounts and reactivities of each.

$$\beta_{tot} = \frac{(k_{AR} + k_{AS})[A]\beta_A + (k_{IR} + k_{IS})[I]\beta_I}{(k_{AR} + k_{AS})[A] + (k_{IR} + k_{IS})[I]} \quad (5)$$

If we now introduce g as the instrinsic reactivity difference between the two states with $g = (k_{IR} + k_{IS})/(k_{AR} + k_{AS})$, then the expression for β_{tot} in eq 5 simplifies further to $\beta_{tot} = ([A]\beta_A + g[I]\beta_A)/([A] + g[I])$. Finally, if A and I are at equilibrium throughout the course of polymerization (i.e., $[A] = K_{eq}[I]$, Scheme 4) then the expression shown in eq 6 results.

This can be recast into more familiar terms if we define the probability for insertion from the isospecific state (regardless of stereochemistry) as shown in eq 7. Substitution into eq 6 then gives the very simple expression for the probability of a single R-placement shown in eq 8.

$$\beta_{tot} = \frac{K_{eq}\beta_A + g\beta_I}{K_{eq} + g} \quad (6)$$

$$P = \frac{(k_{IR} + k_{IS})[I]}{(k_{IR} + k_{IS})[I] + (k_{AR} + k_{AS})[A]} = \frac{g[I]}{g[I] + [A]} = \frac{g[I]}{g[I] + K_{eq}[I]} = \frac{g}{g + K_{eq}} \quad (7)$$

$$\beta_{tot} = (1 - P)\beta_A + P\beta_I \quad (8)$$

From the expression summarized in eq 6, the microstructure of PP produced using a two-state catalyst of this type is sensitive to (at least) four kinetic/thermodynamic parameters (β_A, β_I, g and K_{eq}) even under this specific (and simplifying) set of conditions. While the three parameter expression in eq 8 could be used to derive appropriate expressions for pentad intensities assuming e.g. a site-control model,[4c] it should be clear that an intimate understanding of how such catalysts function requires information on the both the stereoselectivity of insertion from each state, in addition to their relative reactivity/stability.

Nevertheless, eq 6 provides a useful framework for thinking about two-state catalysts of the type discussed here. Suppose that the isopecific state is both more reactive ($g \gg 1$) and stable ($K_{eq} \ll 1$) with $\beta_I > \beta_A$. In the limit (i.e. $g \gg K_{eq}$, $g\beta_I \gg K_{eq}\beta_A$), β_{tot} will become equal to β_I and the unsymmetrical catalyst will behave just like a C_2-symmetrical, isospecific catalyst, i-PP will be produced, and as mentioned previously, there are a number of examples in the literature of such behavior.[8] The converse situation leads to the production of a-PP (assuming $\beta_A = 0.5$); we are not aware of any examples of this in the literature but it might be instructive to try and devise such a catalyst system.

An interesting example is provided by $Me_2C(3\text{-}^tBuCp)(Flu)ZrCl_2$,[8c] in which one of the lateral sites is *very* sterically congested compared to the other, unlike the situation studied here. In this case, both states are isospecific (presumably to different extents) and have the same facial selectivity for monomer insertion (see eq 9). One would expect that the preferred state would

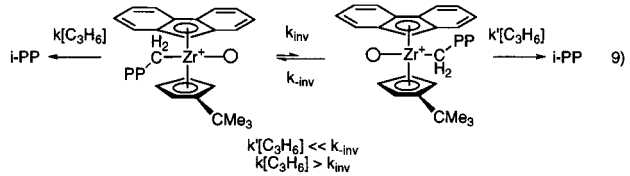

be the one where the polymer chain is located at the less hindered site; one suspects that following migratory insertion (which would generate the less stable state), the polymer chain migrates rapidly back to its thermodynamically preferred location and so to a first approximation, insertion from the other state never competes, i.e., $g = 0$ and therefore $\beta_{tot} \sim \beta_A$ (in this case, the value of $\beta_A \sim 1$).

If both states are of equal stability ($K_{eq} = 1$), but the isospecific state is more reactive, then β_{tot} will always be less than β_I (providing $\beta_I > \beta_A$), the difference between the two being governed by the magnitude of g; similar arguments pertain to the case where there is no difference in reactivity ($g = 1$) but $K_{eq} < 1$ (i.e., the isospecific state is more stable). Finally, if both states are of equal reactivity and stability ($g = K_{eq} \sim 1$), then

Table 3. Physical and Tensile Properties of PP Prepared Using *rac*-6

								elastic recovery		
entry	cond[a]	M_w[b] (K)	mmmm[c] (%)	ΔH_f[d] (J/g)	N_{iso}[e]	stress[f] (MPa)	strain[f] (%)	100%	200%	break
1	10	78.2	35	7	8.3	5.2	1100	97	97	79
2	12	53.5	46	38	10.2	9.9	950	96	95	74
3	8	52.1	48	50	11.9	15.0	1000	88	76	66
4	13	55.9	42	25	8.9	8.9	830	93	97	67
5	11	37.0	49	58	10.5	7.7	390			
6	[g]	50.0	54	40	10.8	16.0	1000	92	90	80
7	[g]	30.0	38	15	8.2	3.0	200			

[a] The number corresponds to entries in Table 2. [b] Determined by GPC. [c] Determined by ^{13}C NMR spectroscopy. [d] Determined by DSC. [e] Average length of isotactic blocks as estimated by ^{13}C NMR spectroscopy, where $N_{iso} = 4 + 2[mmmm]/[rmmm]$. [f] At break. [g] From ref 4b.

the total stereoselectivity will simply be the numerical average of the two individual selectivities.

Clearly, quite variable behavior is expected even for a system where Curtin−Hammett conditions apply. If the rates of state-to-state interconversion via chain migration are faster than the *slowest* propagation step and of the same (or lower) magnitude as that of the *fastest* propagation step, i.e., non-Curtin−Hammett conditions, then the microstructure of the polymer will still be dominated by the state with the faster propagation step (e.g., the isospecific one); however, the microstructure will now be dependent on monomer concentration as observed here (and elsewhere), being *lower* at higher propylene concentration (i.e., an increased tendency to form hemi-isotactic PP). In effect, at high monomer concentration, the least reactive state is kinetically trapped; monomer coordination prevents its isomerization to the more reactive state (via chain inversion) and thus increases the overall likelihood for aspecific insertion. The behavior is quite different from that observed using oscillating catalysts where higher monomer concentrations lead to *more* stereoregular polymer.[5,15]

This picture, which we believe to be qualitatively correct, does not explain how an elastomeric network would be produced. As pointed out before,[4] there will be both an average length (and distribution) of atactic and isotactic block lengths with such catalysts, regardless of the propagation model used to describe the microstructure of elPP. From a practical point of view, if the number of isotactic sequences of sufficient length to cocrystallize is a small fraction of the number of isotactic (and atactic) sequences present in a single polymer chain, one could still generate an elastomeric network, even if the microstructure is not truly blocky as with, e.g., oscillating catalysts.

Elastomeric Properties of Poly(propylene) Prepared Using Catalyst 6. Tensile tests on compression moulded samples of various polymers prepared using catalyst **6** were conducted according to previously published procedures and the results are summarized in Table 3 and typical stress−strain curves are depicted in Figure 4. The properties of these materials are similar to those reported earlier.[3,4]

Some interesting trends in elastomeric behavior in terms of polymer MW and crystallinity can be discerned from these results. For entries 1−5 of Table 3, polymer crystallinity (ΔH_f) was found to be roughly proportional to %mmmm although the lower molecular weight samples tended to exhibit higher crystallinity than expected which may be due to increased mobility of the shorter chain segments (compare entries 2 vs 5). The polymers produced by *rac*-**6** are comparable to those produced by **2** (M = Hf, X = C, Si) where the average

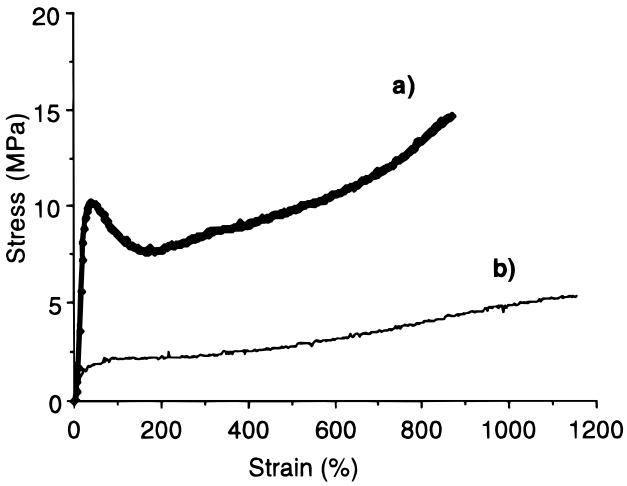

Figure 4. Typical tensile behavior of semicrystalline polypropylenes of variable crystallinity and molecular weights: (a) %mmmm = 47.5, M_w = 52.1 K;(b) %mmmm = 35.1, M_w = 78.2 K.

isotactic block lengths are short (8−12 monomer units in length) as estimated by N_{iso} (Table 3). Generally, the ultimate strength of the polymers was found to be proportional to %mmmm, although in some cases the values reported are somewhat lower than expected (entries 4 and 5 vs 1−3). Although the lower molecular weight samples were of higher ultimate strength, they were generally brittle materials that exhibited low elongations to break and inferior (if any) elastic properties. Higher MW polymer of lower tacticity (which correlates roughly with total crystallinity in these materials) exhibited properties associated with classical elastomers—i.e., low initial modulus, high elongations to break and good elastic recovery. Some of the lower MW, but more stereoregular, polymers exhibited higher initial moduli, yielding behavior (Figure 4), shorter elongations to break, and poorer elastic recovery. The properties of some of these materials are intermediate between classical elastomers and thermoplastics.

We have suggested previously that the structural differences between elPP prepared using catalysts of this type and, e.g., isotactic PP are not as profound as one might envisage based on a true stereo-block microstructure. The gradation in physical properties observed here, which is reminiscent of more random materials, is consistent with this hypothesis. Moreover, these materials feature two different crystallization processes with markedly different rates; the higher melting endotherm develops rapidly from the melt (as revealed by either time dependent differential scanning calorimetry or dynamic mechanical analysis measurements)[4a] while the lower melting process de-

velops much more slowly (days or even weeks at room temperature) and has a pronounced (and negative) effect on elastic properties with time, particularly in the more stereoregular polymers.

Conclusions

From a practical point of view, elPP prepared using unsymmetrical metallocene catalysts should ideally be of higher MW and, perhaps, lower average isotacticity than many of the samples studied here. As mentioned above, the first requirement can probably be easily met by incorporating many of the design features found in high-performance catalysts for production of high MW, isotactic PP. Our results, to date, suggest that what is required is a catalyst with an aspecific state which has comparable (or perhaps greater) stability/reactivity to the isospecific state; modeling studies, regardless of the model employed, suggest that in all other known systems of this type, the converse is true and may indirectly account for the undesirable, 2° crystallization behavior of these materials.

A key requirement of higher peak melting temperatures in elPP necessitates that when crystallizable sequences are produced, they be free of internal defects and do not (readily) cocrystallize with shorter, less perfect sequences on other polymer chains. This may be difficult to achieve using catalysts of this type but might be through melt-processing or in-reactor blending with, e.g., i-PP. In any event, given the high T_g (ca. −15 °C) of atactic PP, elPP has serious limitations as an elastomer that will not be readily solved through advances in catalyst design.

Experimental Section

General Synthetic and Characterization Procedures. Diethyl ether, hexane, THF and toluene were distilled under N_2 from Na and benzophenone prior to use. Dichloromethane was distilled from CaH_2. Reagent grade chemicals were used in all cases and purified if necessary prior to use. All manipulations with air-sensitive compounds were performed using standard Schlenk techniques[16] under N_2 that was previously deoxygenated and dried through a column containing a BASF R3-11/4 Å molecular sieve mixture. Air- or moisture-sensitive compounds were stored in either a Vacuum Atmospheres glovebox or a Braun MB 150M glovebox. Alkyllithium reagents were titrated immediately prior to use following the procedure developed by Lipton.[17] Solid MAO was prepared by evaporation to dryness of a toluene solution of poly(methylaluminoxanes) purchased from Akzo Chemicals Ltd. (9.6 wt % Al in toluene; PMAO/*Tol-781). The complexes $ZrCl_4 \cdot 2THF$[18] and $Zr(NMe_2)_4$[19] were synthesized using known procedures. Solid indenyl- and 1-methylindenyllithium were prepared by the addition of ^{n}BuLi (as a solution in hexanes) to a solution of the corresponding hydrocarbon at −78 °C (THF or Et_2O, respectively). Upon warming the mixture slowly to room temperature, removal of the solvent, and washing the solid with hexane, the pale yellow salts could be obtained in 86−91% yield.

^{1}H and ^{13}C NMR spectra of compounds were obtained on Bruker AM-250 or AC-200 spectrometers in the appropriate deuterated solvent. Chemical shifts were referenced to residual undeuterated solvent. IR spectra were recorded on a Bomem MB100 FT-IR instrument. High-low-resolution mass spectra were measured on a VG 70/70 SE at the WATSPEC facility, University of Waterloo. Elemental analyses were performed by M. H. W. Laboratories of Phoenix, AZ.

Preparation of 3-Methylindene.[20] Indene (17.71 g, 0.1524 mol) was dissolved in 50 mL of THF and cooled to −78 °C. To this solution was added *n*-butyllithium (2.5 M in hexane, 64 mL, 0.160 mol) dropwise over 2.5 h. The solution was allowed to warm very slowly to room temperature over 7 h. In a separate flask, a solution of MeI was prepared by dissolving MeI (19 mL, 0.305 mol) in 20 mL of THF, and the solution was then cooled to −78 °C. The indenyllithium solution was added to the iodomethane solution over 3 h during which time LiI precipitated. Following warming to room temperature (over 3 h), a light yellow solution with a dense white precipitate was obtained. The reaction mixture was extracted twice with an equal volume of hexane. The organic layer was separated and extracted with 100 mL of deionized water and then brine. The organic phase was dried over anhydrous $MgSO_4$, filtered through Celite, and concentrated in vacuo. Further purification was achieved by fractional distillation (80 °C, 10 mmHg) and provided 3-methylindene as a clear, colorless liquid (16.54 g, 83%). The product was dried by vacuum distillation from $LiAlH_4$ prior to use in subsequent reactions. The ^{1}H NMR spectrum of the resulting product was consistent with literature values for 3-methylindene although a small quantity of 1-methylindene was detected as a minor product. For 3-methylindene: ^{1}H NMR (250 MHz, $CDCl_3$) δ 7.57−7.20 (m, 4H, C4−C7), 6.82 (d, 1H, C1), 6.49 (d, 1H, C2), 3.58 (q, 1H, C3), 1.43 (d, 3H, CH_3). For 1-methylindene**:** ^{1}H NMR (250 MHz, $CDCl_3$) δ 7.36 (d, 1H, C8), 7.32−7.06 (m, 3H, C4−C7), 3.20 (m, 2H, C3), 2.07 (d, 3H, CH_3).

Preparation of (3-Methyl-1-indenyl)(1-indenyl)dimethylsilane (4). 1-Methylindenyllithium (4.218 g, 31 mmol) was dissolved in 50 mL of diethyl ether. In a separate flask, Me_2SiCl_2 (18.8 mL, 155 mmol) was dissolved in 50 mL of diethyl ether and cooled to 0 °C. The 1-methylindenyllithium solution was added dropwise to the silane solution dropwise over 6 h. The reaction mixture was allowed to stir at room temperature for at least 2 h. The crude dimethyl(3-methyl-1-indenyl)-chlorosilane was used directly following removal of excess Me_2SiCl_2 and solvent in vacuo. ^{1}H NMR (250 MHz, $CDCl_3$) δ 7.60 (d, 1H), 7.2−7.4 (m, 3H), 6.13 (s, 1H), 3.52 (m, 1H), 2.13 (s, 3H), 0.12 (s, 3H), 0.07 (s, 3H).

The product was redissolved in 60 mL of diethyl ether and cooled to 0 °C. Indenyllithium (3.78 g, 40 mmol) was dissolved in 70 mL of diethyl ether in a separate flask and added slowly to the chlorosilane over a period of 4 h. The solution was left to warm to room temperature, with continuous stirring, overnight. The reaction was quenched by the addition of an equal volume of saturated aqueous NH_4Cl. The crude reaction mixture was extracted with an equal volume of diethyl ether (2×), and the organic phase washed with deionized water (1×), and brine (2×). The combined organic portion was dried over anhydrous $MgSO_4$ and filtered. The final product was obtained as a viscous, clear yellow oil (7.32 g, 78%) as a 1:1 mixture of stereoisomers ((±)-[1*S*,1′*S*] and (±)-[1*S*,1′*R*]) following removal of the solvents in vacuo. Where necessary, purification was achieved by Kugelrohr distillation (110 °C, 0.038 mmHg). The compound was used without prior separation of the isomers in subsequent reactions. IR (NaCl, thin film): 3060, 3012, 2961, 2909, 1940, 1901, 1720, 1602, 1451, 1380, 1359, 1251, 1249, 1187, 1111, 1027, 978, 934, 674, 804, 767, 716, 633 cm^{-1}. ^{1}H NMR (250 MHz, $CDCl_3$) δ For (±)-[1*S*,1′*R*]-**4**: 7.49−7.14 (m, 8H, C4−C7 and C4′−C7′), 6.90 (pseudo-t, J = 5 Hz, 1H, H_3′), 6.62 (m, 1H, H_2′), 6.30 (s, 1H, H_2), 3.61 (m, 2H, H_1), 3.51 (m, 1H, H_1′), 2.24 (m, 3H, CH_3−Ind), −0.11 (s, 3H, CH_3−Si), −0.48 (s, 3H, CH_3−Si). For (±)-[1S,1′S]-**4:** 7.49−7.14 (m, 8H, C4−C7 and C4′−C7′), 6.90 (pseudo-t, 1H, J = 5 Hz, H_3′), 6.43 (m, 1H, H_2′), 6.16 (s, 1H, H_2), 3.61 (m, 1H, H_1), 3.51 (m, 1H, H_1′), 2.22 (m, 3H, CH_3−Ind), −0.28 (s, 3H, CH_3−Si), −0.33 (s, 3H, CH_3−Si). MS(FAB) m/z 302 (M^+). Anal. Calcd for $C_{21}H_{22}Si$: C, 83.38; H, 7.33. Found: C, 83.57; H, 7.35.

Preparation of *meso*-5 and *rac*-6 from $ZrCl_4$. Compound **4** (3.278 g, 10.84 mmol) was dissolved in 30 mL of anhydrous THF. A 3-fold excess of KH (1.034 g, 32.51 mmol) was weighed in the glovebox and slurried in 20 mL of THF. An ultrasonic bath operating at ambient temperature was then used to disperse the solid. The KH slurry was cooled to 0 °C prior to the slow addition (45 min) of the ligand solution. The dianion solution was then allowed to warm to room temperature over 1 h at which time the color changed to a deep forest

green. To ensure the completion of the reaction, the solution was then subject to three 10 min cycles of sonication, followed by stirring.

The dianion solution was isolated from the excess KH by decanting the solution via cannula into a Schlenk frit fitted with a septum, and then filtered by gravity through Celite. Following filtration, the final volume of the dianion solution was brought to 100 mL of THF in a vessel that was previously calibrated for this specific volume. In a separate flask, an equimolar amount of $ZrCl_4$•2THF (4.088 g, 10.84 mmol) was weighed and dissolved in 100 mL of THF. To a third flask, 150 mL of dry THF was added and cooled to room temperature. The reaction was initiated by carefully starting the simultaneous dropwise addition of the $ZrCl_4$•2THF solution and then the dianion solution into a third flask (containing only the solvent) with vigorous stirring while avoiding a local excess of the dianion at any given time.[9c] During the course of the reaction a bright orange or rust-colored solution was obtained with the formation of KCl. The addition of the reagents generally proceeded for at least 6 h and the mixture was stirred overnight at room temperature.

The solvent was removed in vacuo (10^{-3} mmHg). The subsequent manipulations were performed in the glovebox. The crude product was loaded onto a coarse frit and washed freely with hexane and then a minimal volume of toluene, allowing the residue to dry completely between solvents. The residue on the frit (an orange paste) was then extracted with dry CH_2Cl_2 and filtered through dry Celite and the filtrate was concentrated in vacuo to dryness. A ^{1}H NMR spectrum of the bright orange solid residue revealed the formation of two isomers in a 1:1 ratio. Further purification of the isomer mixture was achieved by dissolving the crude product in toluene, followed by recrystallization at −37 °C in fair yields (3.19 g, 64%). The separation of the two isomers was achieved by repeated fractional recrystallization from toluene (−37 °C) in 5−10% and 20−25% overall yields of *rac*-**6** and *meso*-**5**, respectively. The least soluble of the two isomers, *meso*-**5**, is invariably the major product in the first stage of the recrystallization and is isolated first. *rac*-**6** can then be obtained from the enriched filtrate by subsequent recrystallizations, but it is usually contaminated with *meso*-**5**.

meso-**5**. IR (KBr pellet): 3422, 1618, 1400, 1255, 1212, 1128, 964, 831, 808, 788, 738, 676, 644 cm^{-1}. ^{1}H NMR (300 MHz, $CDCl_3$): δ 7.56−7.53 (m, 2H), 7.46−7.40 (m, 2H), 7.18 (t, J = 8 Hz, 2H), 7.04 (d, J = 3 Hz, 1H), 6.91 (m, 2H), 5.92 (d, J = 3 Hz, 1H), 5.64 (s, 1H), 2.40 (s, 3H), 1.35 (s, 3H), 0.90 (s, 3H).^{13}C NMR (300 MHz, CD_2Cl_2) δ 134.7, 134.5, 130.6, 128.7, 128.6, 127.4, 126.7, 126.6, 126.5, 126.6, 126.1, 125.4, 124.3, 119.4, 119.0, 118.8, 89.7, 86.9, 13.7, −0.767, −2.659. MS (EI) m/z 460 (M^+, $^{28}Si^{35}Cl_2{}^{90}Zr$). Anal. Calcd for $C_{21}H_{20}SiCl_2Zr$: C, 54.52; H, 4.36. Found: C, 54.60; H, 4.37.

rac-**6**. IR (KBr pellet): 3385, 1609, 1523, 1435, 1401, 1368, 1343, 1259, 1210, 1143, 1126, 834, 819, 748, 681, 644 cm^{-1}. ^{1}H NMR (200 MHz, $CDCl_3$) δ 7.58 (dt, J = 8 Hz, J = 1 Hz, 1H), 7.48−7.25 (m, 5H), 7.05 (m, 2H), 6.91 (dd, J = 2 Hz, J = 5 Hz, 1H), 6.10 (d, J = 3 Hz, 1H), 5.70 (s, 1H), 2.33 (s, 3H), 1.11 (s, 3H), 1.08 (s, 3H).^{13}C NMR (300 MHz, CD_2Cl_2): δ (ppm) 134.3, 133.7, 128.6, 127.7, 127.3, 127.1, 127.0, 126.3, 126.3, 125.4, 125.0, 124.6, 118.7, 118.0, 117.3, 89.6, 86.3, 13.6, −1.1, −1.4, −2.7. MS (EI), m/z 460 (M^+, $^{28}Si^{35}Cl_2{}^{90}Zr$) . Anal. Calcd for $C_{21}H_{20}SiCl_2Zr$: C, 54.52; H, 4.36. Found: C, 54.67; H, 4.40.

Preparation of *rac*-6 via Amine Elimination. $Zr(NMe_2)_4$ (641 mg, 2.39 mmol) was dissolved in 35 mL of hexane in a three-neck round-bottom flask at room temperature. In a separate flask, **4** (724 mg, 2.39 mmol) was dissolved in 20 mL of hexane. The $Zr(NMe_2)_4$ solution was cooled to approximately −78 °C prior to the addition of the solution of **4**. The reaction mixture was then allowed to warm to room temperature and stirred for 2 h during which a color change was observed from light yellow to orange.

The next step of the synthesis required refluxing of the reaction mixture for a period of 10 h. The flask was fitted with a Vigreux column, a water-cooled reflux condenser, and a three-way stopcock which vented to an oil bubbler. During the course of the reaction, N_2 was purged through the reaction vessel through a stopcock gas inlet fitted to the round-bottom flask. These steps were taken to remove NMe_2H from the reaction mixture more efficiently and minimize solvent loss during reflux. After 10 h, the reaction mixture was cooled to room temperature and then the solvent was removed in vacuo yielding an isomeric mixture of products as an orange-red viscous oil.

Due to the complexity of the product mixture obtained, the dimethylamido complexes were not purified. However, the degree of completion of the reaction was verified by obtaining an ^{1}H NMR spectrum of the crude product in C_6D_6. Key spectral indicators include the disappearance of ligand and $Zr(NMe_2)_4$ resonances (δ 2.96) and an upfield shift of the methyl signal of $Zr(NMe_2)_4$ upon complexation to the metal from δ 2.96 to 2.46.

The dimethylamido complexes were converted to the dichlorides by reaction of with excess (10 equiv) trimethylchlorosilane (2.60 g, 23.9 mmol) in toluene at room temperature. Following the addition of the trimethylchlorosilane, the reaction mixture was allowed to stir overnight. The volatiles were removed in vacuo to yield a rust-colored solid. In the glovebox, the solid was transferred to a frit and washed freely with hexane until the filtrate was colorless. The final product was recrystallized from toluene (−37 °C) to give a bright orange solid in (60% yield, 663 mg) with a *rac*-**6**:*meso*-**5** isomer ratio of 6:1. Repeated fractional recrystallization from toluene gave pure *rac*-**6** in 36% overall yield based on the starting materials.

Polymerization Procedures and Polymer Characterization. Propene Polymerizations. Propene polymerizations were conducted in a 1 L Autoclave Engineers Zipperclave reactor. Temperature was controlled using a Neslab RTE-110 constant temperature bath by circulation of coolant (50:50 v/v ethylene glycol:water) through an external jacket. The temperature was monitored/controlled with a Neslab RS-2 remote sensor using a Pt RTD sensor immersed in a thermowell inside the reactor. The consumption of monomer during the course of the polymerization was followed using a calibrated Matheson mass flow controller which was controlled by a Matheson Dynablender Model 8219 power supply/readout. The data (temperature, flow of monomer) were input and stored into a computer that was equipped with a PCL-711S data acquisition card that used analogue voltage as input. The progress of the polymerization was monitored in real time using Labtech Acquire data acquisition software which converted the digital input readings to the desired values (°C, and mL/min of C_3H_6) using appropriate conversion factors. For kinetic analyses, the $[C_3H_6]$ in toluene was calculated from the mole fraction of toluene ($X_{C_3H_6}$) for a specific temperature (T, °C) and pressure using the following relationships: (a) for 15 psi, $X_{C_3H_6} = 0.179 - (3.37 \times 10^{-3})\ T + (1.83 \times 10^{-5})\ T^2$; (b) for 30 psi, $X_{C_3H_6} = 0.354 - (6.75 \times 10^{-3})\ T + (3.66 \times 10^{-5})\ T^2$; (c) for 45 psi, $0.536 - (1.01 \times 10^{-2})\ T + (5.49 \times 10^{-5})\ T^2$.[21] All gases were purified by passage through a stainless steel tower filled with a R3-11 catalyst and 4 Å molecular sieve mixture for removal of moisture and oxygen. The purified gases were then fed through 40 μm in-line filters to eliminate foreign particles.

Prior to each polymerization the reactor was cleaned and dried by stirring (at 800 rpm) with 600 mL of a 2.0 M solution of trimethylaluminum in toluene. This solution was expelled from the reactor followed by purging with dry N_2. In the glovebox, the desired amount of MAO ([Al]:[Zr] = 2000:1, 621 mg) was loaded into a 50 mL sample bomb. The MAO was flushed into the reactor with 500 mL of toluene. For each run, the cocatalyst solution (MAO/toluene) was presaturated with the monomer at the specified pressure. Initially, the reactor was equilibrated to within 1−2 °C of the desired temperature before the introduction of monomer.

The polymerization was initiated by the addition of the catalyst as a toluene solution in one of two ways: syringe injection or sample vessel. Typically this solution was prepared by dissolving 3−4 mg of the catalyst in a minimum amount of solvent with stirring under N_2. An aliquot of this solution was obtained so that in all cases 5 μmol of Zr was injected into the reactor in a typical run. For experiments conducted at higher pressures (e.g., 45 psi) a more convenient

method of catalyst delivery was employed whereby the aliquot was loaded into the sample bomb and diluted with 15 mL of toluene in the glovebox. Outside the glovebox, this solution was delivered into the reactor using N_2 pressure. The reaction was quenched by injecting 2−3 mL of methanol and quickly venting the monomer.

Polymer Isolation and Characterization. General. The bulk of the solvent was removed in vacuo. The polymers were then deashed by stirring for several hours with 40 mL of a 2.0 M solution of HCl in methanol, followed by drying for at least 15 h at 70 °C and 0.01 mmHg. ^{13}C NMR analyses were performed on these unfractionated polymers. The insoluble catalyst residues were separated from the polymer by Soxhlet extraction from refluxing toluene for at least 12 h so that all polymer fractions regardless of molecular weight and crystallinity were dissolved. The extractions were continued until the residues attained constant weight, often for at least 24 h. Polymer solutions were then concentrated in vacuo and dried prior to use for differential scanning calorimetry (DSC), gel permeation chromatography (GPC), and tensile testing.

^{13}C NMR Spectra of PP Samples. The NMR samples were prepared in a 10 mm o.d. tube by dissolving 500−700 mg of polymer in 1,2,4-trichlorobenzene containing 0.1% BHT. Frequency-field locking was accomplished by the addition of a few drops of C_6D_6 to the sample prior to transfer to the probe. Spectra were acquired on a Bruker AMX-300 that had been equilibrated and shimmed using DMSO-d_6 at 120 °C. The samples were equilibrated for at least 45 min prior to the adjustment of the nonspinning shims. A typical experiment employed a 30° pulse width and inverse-gated decoupling over a 160 ppm spectral width. Under these conditions, typically 4000−6000 transients were sufficient for good signal to noise ratio (S/N), although longer acquisition times were necessary for the less soluble, higher molecular weight samples. In the case of low molecular weight polymer samples, the number average degree of polymerization M_n was estimated from the ratio of the total methyl pentad intensity to the methyl of the *n*-propyl end group and corrected for overlapping end group and regioirregularity signals where necessary.[22]

DSC Analyses. The polymer samples (10−12 mg) were weighed and sealed in aluminum pans. The sealed samples were melted by heating at a controlled rate (5 °C/min) from room temperature up to 120 °C and held at this temperature for 30 min to destroy all prior thermal history. The crystallites were then allowed to re-form slowly as the polymer samples were cooled back to room temperature at a controlled rate (0.5 °C/min). The samples were held at room temperature for 4 days prior to analysis.

The analyses were performed on a Perkin-Elmer DSC that had previously been calibrated using indium. The values reported are for the annealed polymer samples which were heated from 273 to 393 K at a heating rate of 10 °C/min at the 10 mcal/s setting. At the end of the first run, the polymer samples were cooled at a rate of 1.25 °C/min back to 273 K and the experiment was repeated under the same conditions. The data were recorded for both runs for comparison.

GPC Analyses. Unless otherwise indicated, polymer molecular weights and distributions were determined by gel permeation chromatography (GPC) using a Waters 150C chromatograph employing both a differential refractive index and a differential viscometer as detectors. The GPC was operated at 145 °C using 1,2,4-trichlorobenzene with 0.1% BHT as antioxidant for elution and the samples were prepared from 1 to 2 mg of polymer/mL of TCB. Sample dissolution was accomplished by rotating the samples in an oven operating at 160 °C for a period of 2 days. Narrow molecular weight distribution, polystyrene standards were used for calibration.

Tensile Testing. The specimens used for tensile testing were prepared from the extracted polymers (typically 300 mg of polymer/sample) by compression molding at 20 000 lbs, and 120 °C. Once molded the samples were cooled slowly to room temperature and annealed at that temperature for at least 3 days prior to analysis. The dumbbell-shaped specimens were prepared according to ASTM D412 (0.32 cm × 2.75 cm × 0.16 cm, with a gauge length of 0.80 cm). The analyses were done on an Instron tensile tester at a strain rate of 25.5 cm/s using a gauge length setting of 15 mm on the instrument. For each polymer sample, an average of at least three trials was used. For each sample, a set of benchmarks of about 5 mm in separation were first inscribed in the middle (narrow) section of each of the dumbbell-shaped specimens and this distance was measured to give L_i. The ultimate strength and percent elongation (to break) were determined for each specimen by elongating the sample to the point of breakage; data collection [force (N) vs time (s)] was computer controlled. To determine the ultimate strength of the polymer, the sample cross-sectional area was initially measured with a pair of calipers for each specimen. The ultimate strength (MPa) of the polymers was calculated as the force (N) at the breakage point divided by the cross-sectional area (A, mm^2). The time of the elongation, t (s), was multiplied by the strain rate (25.5 cm/s) and then added to the original gauge length (l_o) to give the overall length of the sample at time t (l_t). The percent strain was calculated as $100[(l_t - l_o)/l_o]$. For a given strain, the corresponding apparent tensile stress was calculated from the observed force (N), tensile stress (MPa) $= F/A$, under the assumption that A remains constant during the course of the experiment. After the point of breakage and following a 30 s recovery interval, the gauge length was measured to determine L_r. The elastic recovery at break was calculated as % recovery $= [(L_m - L_r)/(L_m - L_i)] \times 100$, where $l_t = L_m$ and $l_o = L_i$. The elastic recovery at lower values of strain (100, 200%) was similarly calculated following elongation of the specimen to the prescribed benchmark distance.

Acknowledgment. The authors thank the Natural Sciences and Engineering Research Council of Canada and Novachem Chemicals, Ltd., of Calgary, Alberta, Canada, for financial support of this work. We are also grateful to W. J. Gauthier for his helpful contributions and informative discussions.

References and Notes

(1) (a) Natta, G. *J. Polym. Sci.* **1959**, *34*, 531. (b) Natta, G.; Mazzanti, G.; Crespi, G.; Moraglio, G. *Chim. Ind., Milano* **1957**, *39*, 275.

(2) (a) Tullock, C. W.; Mülhaupt, R.; Ittel, S. D. *Makromol. Chem., Rapid Commun.* **1989**, *10*, 19. (b) Tullock, C. W.; Tebbe, F. N.; Mülhaupt, R.; Ovenall, D. W.; Setterquist, R. A.; Ittel, S. D. *J. Polym. Sci., Polym. Chem.* **1989**, *27*, 3063. (c) Collette, J. W.; Ovenall, D. W.; Buck, W. H.; Ferguson, R. C. *Macromolecules* **1989**, *22*, 3858. (d) Collette, J. W.; Tullock, C. W.; MacDonald, R. N.; Buck, W. H.; Su, A. C. L.; Harrel, J. R.; Mülhaupt, R.; Anderson, B. C. *Macromolecules* **1989**, *22*, 3851.

(3) (a) Mallin, D. T.; Rausch, M. D.; Lin, G.-Y.; Dong, S.; Chien, J. C. W. *J. Am. Chem. Soc.* **1990**, *112*, 2030. (b) Chien, J. C. W.; Llinsas, G. H.; Rausch, M. D.; Lin, G.-Y.; Winter, H. H. *J. Am. Chem. Soc.* **1991**, 113, 8569. (c) Chien, J. C. W.; Llinsas, G. H.; Rausch, M. D.; Lin, G.-Y.; Winter, H. H., Atwood, J. L.; Bott, S. G. *J. Polym. Sci., Polym. Chem.* **1992**, *30*, 2601. (d) Llinas, G. H.; Day, R. O.; Rausch, M. D.; Chien, J. C. W. *Organometallics* **1993**, *12*, 1283.

(4) (a) Gauthier, W. J. Ph.D. Thesis, Chemistry Department, University of Waterloo, Waterloo, Ontario, Canada, 1994. (b) Gauthier, W. J.; Corrigan, J. F.; Taylor, N. J.; Collins, S. *Macromolecules* **1995**, *28*, 3771. (c) Gauthier, W. J.; Collins, S. *Macromolecules* **1995**, *28*, 3779.

(5) (a) Coates, G. W.; Waymouth, R. M. *Science* **1995**, *267*, 217. (b) Hauptman, E.; Waymouth, R. M.; Ziller, J. W. *J. Am. Chem. Soc.* **1995**, *117*, 11586. (c) Kravchenko, R.; Masood, A.; Waymouth, R. M. *Organometallics* **1997**, *16*, 3635.

(6) Rieger, B.; Repo, T.; Jany, G. *Polym. Bull.* **1995**, *35*, 87.

(7) (a) Spaleck, W.; Antberg, M.; Dolle, V.; Klein, R.; Rohrmann J.; Winter, A. *New J. Chem.* **1990**, *14*, 499. (b) Spaleck, W.; Antberg, M.; Rohrmann, J.; Winter, A.; Bachmann, B.; Kiprof, P.; Behm, J.; Herrmann, W. A. *Angew. Chem., Int. Ed. Engl.* **1992**, *31*, 1, 1347. (c) Spaleck, W.; Küber, F.; Winter, A.; Rohrmann, J.; Bachmann, B.; Antberg, M.; Dolle, V.; Paulus, E. F. *Organometallics* **1994**, *13*, 954.

(8) (a) Miyake, S.; Okumura, Y.; Inazawa, S. *Macromolecules* **1995**, *28*, 3074. (b) Ewen, J. A.; Elder, M. J. In *Ziegler Catalysts;* Fink, G., Mülhaupt, R., Brintzinger, H.-H., Eds.;

Springer-Verlag: Berlin, 1995; p 107. (c) Razavi, A.; Atwood, J. L. *J. Organomet. Chem.* **1996**, *520*, 115.
(9) (a) Collins, S.; Kuntz, B. A.; Taylor, N. J.; Ward, D. G. *J. Organomet. Chem.* **1988**, *342*, 21. (b) Grossman, R. B.; Doyle, R. A.; Buchwald, S. L. *Organometallics* **1991**, *10*, 1501. (c) Lee, I.-M.; Gauthier, W. J.; Ball, J. M.; Iyengar, B.; Collins, S. *Organometallics* **1992**, *11*, 2115.
(10) (a) Diamond, G. M.; Rodewald, S.; Jordan, R. F. *Organometallics* **1995**, *14*, 5. (b) Christopher, J. N.; Diamond, G. M.; Jordan, R. F. *Organometallics* **1996**, *15*, 4038. (c) Diamond, G. M.; Jordan, R. F.; Petersen, J. L. *Organometallics* **1996**, *15*, 4045. See also Hughes, A. K.; Meetsma, A.; Teuben, J. H. *Organometallics* **1993**, *12*, 1936.
(11) We thank Professor Jordan and his group for disclosing details of these amine elimination reactions prior to publication.
(12) In stereochemically rigid systems such as ansa-zirconocenes, ^{1}H NOE difference experiments provide information on the spatial proximity between protons; providing these signals can be correctly assigned (as is straightforward in this case), structural assignment of stereoisomers is possible. The technique is widely applied in organic chemistry—see: Williams, D. H.; Fleming, I. *Spectroscopic Methods in Organic Chemistry*, 4th ed.; McGraw-Hill, Maidenhead, U.K., 1987; pp 114−118.
(13) For theoretical studies see: (a) Woo, T. K.; Fan, L.; Ziegler, T. *Organometallics* **1994**, *13*, 432. (b) Lohrenz, J. C. W.; Woo, T. K.; Fan, L.; Ziegler, T. *J. Organomet. Chem.* **1995**, *497*, 91. (c) Støvneng, J. A.; Rytter, E. *J. Organomet. Chem.* **1996**, *519*, 227. For related experimental work see: (d) Stehling, U.; Diebold, J.; Kirsten, R.; Roll, W.; Brintzinger, H.-H. *Organometallics* **1994**, *13*, 964. (e) Resconi, L.; Fait, A.; Piemontesi, F.; Colonessi, M.; Rychlicki, H.; Zeigler, R. *Macromolecules* **1995**, *28*, 6667.
(14) (a) Ewen, J. A.; Elder, M. J. *Makromol. Chem., Makromol. Symp.* **1993**, *66*, 179. (b) Ewen, J. A.; Elder, M. J.; Jones, R. L.; Haspelagh, L.; Atwood, J. L.; Bott, S. G.; Robinson, K. *Makromol. Chem., Makromol. Symp.* **1991**, *48/49*, 253.
(15) From a consideration of the mechanism proposed for oscillating catalysts, higher monomer concentration should lead to increased block lengths for both the isotactic and atactic blocks; however the magnitude of the increase will be dependent on both the relative reactivity and amounts of the two-states present during polymerization.
(16) Shriver, D. F.; Drezdon, M. A. *The Manipulation of Air-Sensitive Compounds*, 2nd ed.; Wiley: New York, 1986.
(17) Lipton, M. F.; Sorensen, C. M.; Sadler, A. C. *J. Organomet. Chem.* **1980**, *186*, 155.
(18) Manzer, L. *Inorg. Synth.* **1982**, *21*, 137.
(19) (a) Bradley, D. C.; Thomas, I. M. *Proc. Chem. Soc., London* **1959**, 225. (b) Bradley, D. C.; Thomas, I. M. *J. Chem. Soc.* **1960**, 3857.
(20) Weidler, A. M. *Acta Chem. Scand.* **1963**, *17*, 2724.
(21) The data relationships used were derived by W. J. Gauthier and co-workers at W.R. Grace, Washington Research Center, Columbia, MD.
(22) (a) Zambelli, A.; Locatelli, P.; Bajo, G. *Macromolecules* **1979**, *12*, 154. (b) Zambelli, A.; Locatelli, P.; Rigamonti, E. *Macromolecules* **1979**, *12*, 156. (c) Grassi, A.; Zambelli, A.; Resconi, L.; Albizzati, E.; Mazzochi, R. *Macromolecules* **1988**, *21*, 617. (d) Resconi, L.; Piemontesi, F.; Franciscono, G.; Abis, L.; Fiorani, T. *J. Am. Chem. Soc.* **1992**, *114*, 1025.

MA971325B